

Original Paper

Multivariate natural gas price forecasting model with feature selection, machine learning and chernobyl disaster optimizer

Pei Du^a, Xuan-Kai Zhang^a, Jun-Tao Du^{b,*}, Jian-Zhou Wang^c

^a School of Business, Jiangnan University, Wuxi, 214122, Jiangsu, China

^b School of Statistics & Applied Mathematics, Anhui University of Finance and Economics, Bengbu, 233030, Anhui, China

^c Institute of Systems Engineering, Macau University of Science and Technology, Macau SAR, 999078, China

ARTICLE INFO

Article history:

Received 23 December 2024

Received in revised form

18 September 2025

Accepted 19 September 2025

Available online 24 September 2025

Edited by Jia-Jia Fei

Keywords:

Natural gas price forecasting
Multivariate forecasting model
Machine learning
Chernobyl disaster optimizer

ABSTRACT

The significance of accurately forecasting natural gas prices is far-reaching and significant, not only for the stable operation of the energy market, but also as a key element in promoting sustainable development and addressing environmental challenges. However, natural gas prices are affected by multiple source factors, presenting complex, unstable nonlinear characteristics hindering the improvement of the prediction accuracy of existing models. To address this issue, this study proposes an innovative multivariate combined forecasting model for natural gas prices. Initially, the study meticulously identifies and introduces 16 variables impacting natural gas prices across five crucial dimensions: the production, marketing, commodities, political and economic indicators of the United States and temperature. Subsequently, this study employs the least absolute shrinkage and selection operator, grey relation analysis, and random forest for dimensionality reduction, effectively screening out the most influential key variables to serve as input features for the subsequent learning model. Building upon this foundation, a suite of machine learning models is constructed to ensure precise natural gas price prediction. To further elevate the predictive performance, an intelligent algorithm for parameter optimization is incorporated, addressing potential limitations of individual models. To thoroughly assess the prediction accuracy of the proposed model, this study conducts three experiments using monthly natural gas trading prices. These experiments incorporate 19 benchmark models for comparative analysis, utilizing five evaluation metrics to quantify forecasting effectiveness. Furthermore, this study conducts in-depth validation of the proposed model's effectiveness through hypothesis testing, discussions on the improvement ratio of forecasting performance, and case studies on other energy prices. The empirical results demonstrate that the multivariate combined forecasting method developed in this study surpasses other comparative models in forecasting accuracy. It offers new perspectives and methodologies for natural gas price forecasting while also providing valuable insights for other energy price forecasting studies.

© 2025 The Authors. Publishing services by Elsevier B.V. on behalf of KeAi Communications Co. Ltd. This is an open access article under the CC BY license (<http://creativecommons.org/licenses/by/4.0/>).

1. Introduction

1.1. Research background

Against the backdrop of rapid global industrialization, clean energy plays a crucial role in addressing environmental issues, promoting clean production, and fostering green development

(Zheng et al., 2023; Liang et al., 2024). As an important form of clean energy, natural gas has emerged as one of the most important alternative energy sources for the future (LaPlue, 2022), not only due to its high fuel efficiency, operational flexibility, low capital costs, and environmental benefits, but also because it holds significant strategic importance in accelerating energy transition, optimizing energy consumption structures, and establishing a low-carbon economic system (Javid et al., 2022). Thus, accurate natural gas price forecasting is of great significance for utility planning and operations as well as national economic development (Čeperić et al., 2017). However, natural gas prices are nonlinear and complex (Xie et al., 2023), and are influenced by

* Corresponding author.

E-mail address: 120210063@aufe.edu.cn (J.-T. Du).

Peer review under the responsibility of China University of Petroleum (Beijing).

factors such as supply and demand, exchange rates, macroeconomic policies, extreme weather, wars, and environmental conditions (Shi and Shen, 2021; Li et al., 2021; Zheng et al., 2023). Specifically, long-term trends in natural gas prices are driven by supply and demand, with natural gas inventory levels, production, imports and exports, and consumption having a significant impact on prices (Xia and Li, 2024; Yarlagadda et al., 2024). Temperatures are also correlated with natural gas consumption, which indirectly affects natural gas prices (Li et al., 2022). The impact of the price linkage effect of alternative energy sources, such as crude oil as a core substitute, whose price volatility directly affects natural gas pricing (Perifanis and Dagoumas, 2021). Geopolitical risks, such as the Russia-Ukraine conflict, affect gas prices by triggering price volatility through supply chain disruptions, export restrictions and investment uncertainty (Iliyasu et al., 2025). In addition, exchange rate fluctuations (e.g., EUR/USD, USD/JPY) can also have a nonlinear impact on gas prices due to the cross-border nature of trading gas futures. Therefore, the complex characteristics of natural gas prices and their intricacies pose a great challenge to forecasting natural gas prices accurately.

1.2. Literature review

1.2.1. Linear and nonlinear forecasting models

The linear forecasting model, such as autoregressive moving average (ARMA) model (Ervural et al., 2016), typically rely on assumptions about the statistical distribution and stationarity of the research data, and are unable to capture the nonlinear characteristics of energy prices, resulting in high prediction errors (Gao et al., 2023). However, natural gas price series often exhibit complex nonlinear characteristics, so it is necessary to introduce nonlinear models to improve prediction performance (Xie et al., 2023). For example, Malliaris and Malliaris (2008) utilized linear and nonlinear models to predict energy product prices, finding that nonlinear models yielded lower prediction errors than linear models. Therefore, nonlinear models, particularly artificial intelligence (AI) models such as artificial neural networks (ANNs) (Yang et al., 2023a), support vector regression (SVR) (Xian and Che, 2022), and deep learning models, have become increasingly popular for gas price prediction (Sun et al., 2021), because they can handle nonlinear relationships and achieve high prediction accuracy. Zheng et al. (2023) established an optimized SVR to predict gas price, ultimately validating that nonlinear models outperform linear models in terms of nonlinear fitting capability. However, AI models still face some challenges that need to be addressed, such as overfitting, slow convergence, and local optima, etc. (Niu et al., 2020).

1.2.2. Univariate and multivariate forecasting models

Recently, AI models have been widely applied to energy price forecasting. However, in addition to selecting the appropriate model, whether to adopt a multivariate analysis method remains an issue in this field. Wang et al. (2021) obtained excellent forecasting results using a univariate AI model, but this model was designed for short-term prediction. In general, previous findings have shown that univariate approaches perform satisfactorily in most cases, but their prediction performance tends to be significantly degraded when dealing with long-term prediction tasks and large data fluctuations (Cabello-López et al., 2023; Ziel and Weron, 2018). Meanwhile, more and more researchers and scholars have confirmed that various factors contribute to fluctuations in natural gas prices, such as requirement, prices of other energy products, extreme weather, and geopolitical events, etc. However, existing studies tend to focus on univariate forecasting approaches, which are difficult to effectively capture these

complex patterns behind them and deal with the effects of multiple factors (Ziel and Weron, 2018). Therefore, it is crucial and meaningful to construct a multivariate natural gas forecasting model that considers relevant influencing factors. To our knowledge, only a limited number of studies have developed multivariate natural gas price forecasting models and achieved a certain degree of improvement in accuracy (Su et al., 2019; Guan et al., 2022; Li et al., 2021; Zheng et al., 2023). However, these researches only introduced multivariate models and did not compare them with univariate models. Thus, drawing on experience from other energy market studies, it is necessary to simultaneously develop both univariate and multivariate methods and further explore the impact of multivariate models on the accuracy through comparison (Ziel and Weron, 2018).

1.2.3. Individual, hybrid and combined models

Individual models are simple models based on different prediction principles that achieve prediction by modeling historical data sequences (Wang et al., 2017). However, researchers have progressively confirmed that each model has its own strengths and weaknesses, with no single model inherently superior to others (Guo et al., 2011). Especially considering the uncertainty, dynamism, and nonlinear characteristics exhibited by energy prices (Du et al., 2018), a single model struggles to effectively capture specific patterns within the data and achieve accurate predictions (Niu et al., 2022). As a result, hybrid forecasting models and combined forecasting models have emerged (Hao et al., 2023). Hybrid models have become a leading approach in energy price forecasting, combining data preprocessing, predictive methods, optimization techniques, and feature selection to enhance accuracy. They have been applied in time series prediction across diverse domains (Niu and Wang, 2019; Jiang et al., 2023; Wu et al., 2022). For instance, Lin et al. (2022) validated the effectiveness and reliability of the developed hybrid forecasting model in predicting natural gas and carbon futures prices. However, hybrid models are typically based on a single forecasting model, and their forecasting performance is limited by the inherent shortcomings of the single model (Hao et al., 2023). In contrast, the combined model primarily combines different types of forecasting models to ultimately achieve superior forecasting results by integrating the advantages of multiple forecasting models. Jiang et al. (2023) proposed a novel combined forecasting model by combining backpropagation, bidirectional long short-term memory networks (BiLSTM), gated recurrent units (GRU), and optimization algorithms, which demonstrated robust forecasting performance. Generally, combined models enhance predictive performance by integrating multiple models and leveraging the advantages of different predictive models to compensate for the shortcomings of single models (Yang et al., 2023b).

1.2.4. Comments

Through the literature survey and combining, the relevant literature reviews are outlined below:

Comment 1: Compared with linear models, nonlinear models are generally recognized by research scholars for their wide application in energy price forecasting. However, there are many types of nonlinear models, each with its own advantages and disadvantages. Therefore, it is still a challenge to construct scientific and effective forecasting models to accurately predict energy prices.

Comment 2: Natural gas prices are affected by a variety of factors, yet most of the existing studies focus on univariate forecasting, making it difficult to effectively capture the complex fluctuation patterns triggered by these factors. To the best of our knowledge, only a few studies have constructed multivariate

natural gas price forecasting models without comparing univariate and multivariate forecasting results. Meanwhile, the neglect of the importance of data on influencing factors may lead to insufficient forecasting accuracy.

Comment 3: Existing research on energy price forecasting indicates that individual models struggle to meet accuracy requirements, and hybrid models based on single models and multiple techniques or combined models using different forecasting models have significant prediction superiority and have become the mainstream research paradigm for energy price prediction. However, most existing literature relies on single-strategy approaches, with limited in-depth exploration of hybrid or combined strategies.

1.3. Innovations and main contributions

According to the analysis and summary of existing literature, this study conducts comparative analyses from multiple perspectives, such as feature selection, univariate and multivariate models, single models, hybrid models and combined models, respectively, to explore their impact on the performance of natural gas price prediction. And finally it proposes an improved combined multivariate forecasting model, which can provide a reference to the prediction and decision-making of natural gas price. This research offers the following innovations and contributions:

- (1) **Proposing a novel combined model with high accuracy and stability.** An improved combined multivariate forecasting model is developed for natural gas price prediction. It combines feature selection (FS) algorithms, Chernobyl disaster optimizer (CDO) and machine learning techniques, including a hybrid model of convolutional neural network (CNN) and long short-term memory (LSTM), i.e., CNN-LSTM and SVR, namely FS-CDO-CNN-LSTM&SVR model. In comparison to the conventional univariate and multivariate models, the developed combined model can demonstrate higher prediction accuracy and stronger prediction stability.
- (2) **Comprehensive consideration and analysis of multi-source influencing factors.** The combined multivariate forecasting model proposed in this study integrates sixteen multi-source influences on natural gas prices, including five dimensions: production, marketing, commodities, political and economic indicators of the United States (U.S.) and temperature. In order to clarify which variable datasets are more effective, three different types of feature selection algorithms are introduced to screen features of the influencing variables to further enhance the performance of natural gas price prediction.
- (3) **Scientific and effective validation of model performance.** Three comparison experiments are designed. Moreover, six univariate prediction comparison models, thirteen multivariate prediction comparison models, involving linear and nonlinear models, single, hybrid and combined models, while several model evaluation criteria, hypothesis testing, stability testing, and improvement ratio from the proposed model are introduced to comprehensively validate the presented combined method. And the final results demonstrate that the combined forecasting method presented in this work has a significant improvement of performance in natural gas price prediction.

The remaining sections of this study are arranged as below. The second section introduces the research framework of this study, the third section is the introduction of methods, the fourth section provides the data description and feature selection, the fifth

section provides the experiments and related results analysis, the sixth section gives further discussions, and the last section offers the conclusion.

2. The research framework of this study

A novel combined multivariate forecasting model combining different feature selection methods, forecasting models and optimization algorithms is developed for natural price forecasting, which mainly consists of five stages: (1) Data collection, (2) feature selection, (3) experiments, (4) model evaluation, and (5) further discussions, as presented in Fig. 1.

- (1) **Data collection:** This section collects natural gas price data and its exogenous variables, including production factor: U. S. total natural gas underground storage capacity (NGUS), gross natural gas withdrawals (NGGW), crude oil and natural gas rotary rigs in operation (NGRR), marketing factor: natural gas imports (NGI), price of natural gas imports (PNGI), natural gas exports (NHE), natural gas consumption (NGTC), commodities: crude oil future (CO), heating oil future (HO), U.S. political and economic indicators: dollar index (DI), geopolitical risk (GPR) index, EUR/USD exchange rate, USD/JPY exchange rate, and temperature data: contiguous U.S. minimum, maximum and average temperatures.
- (2) **Feature selection:** Three feature selection methods, including the least absolute shrinkage and selection operator (LASSO), grey correlation degree (GRA) and random forest (RF), are employed to remove variables that are irrelevant or redundant concerning natural gas prices, ensuring that only the most pertinent features are preserved. Subsequently, the data are normalized to ensure consistency between features.
- (3) **Experiments:** This stage conducts three experiments, including Experiment I: Comparison between univariate and multivariate models, Experiment II: focuses on comparison of multivariate hybrid models, and Experiment III: Evaluation of different optimization algorithms. These experiments aim to highlight the superior predictive performance of the proposed combined forecasting method from various perspectives through comparisons with benchmark models.
- (4) **Model evaluation:** Five statistical metrics are employed to evaluate the forecasting models comprehensively, scientifically, and efficiently. These include mean absolute error (MAE), root mean square error (RMSE), normalized mean square error (NMSE), Theil's inequality coefficient (TIC), and the coefficient of determination (R^2). These metrics assess the models' prediction accuracy, predictive capability, and generalization ability from multiple dimensions.
- (5) **Further discussions:** To further demonstrate the advantages of the proposed prediction model, this section provides a detailed comparison between the developed combined method and the benchmark models, focusing on hypothesis testing, forecasting effectiveness, and improvement ratio (IR).

3. Methods

3.1. Feature selection methods

3.1.1. Least absolute shrinkage and selection operator (LASSO)

LASSO regression (Tibshirani, 1996) is prevalently utilized for dimensionality reduction, incorporates the penalty function. This

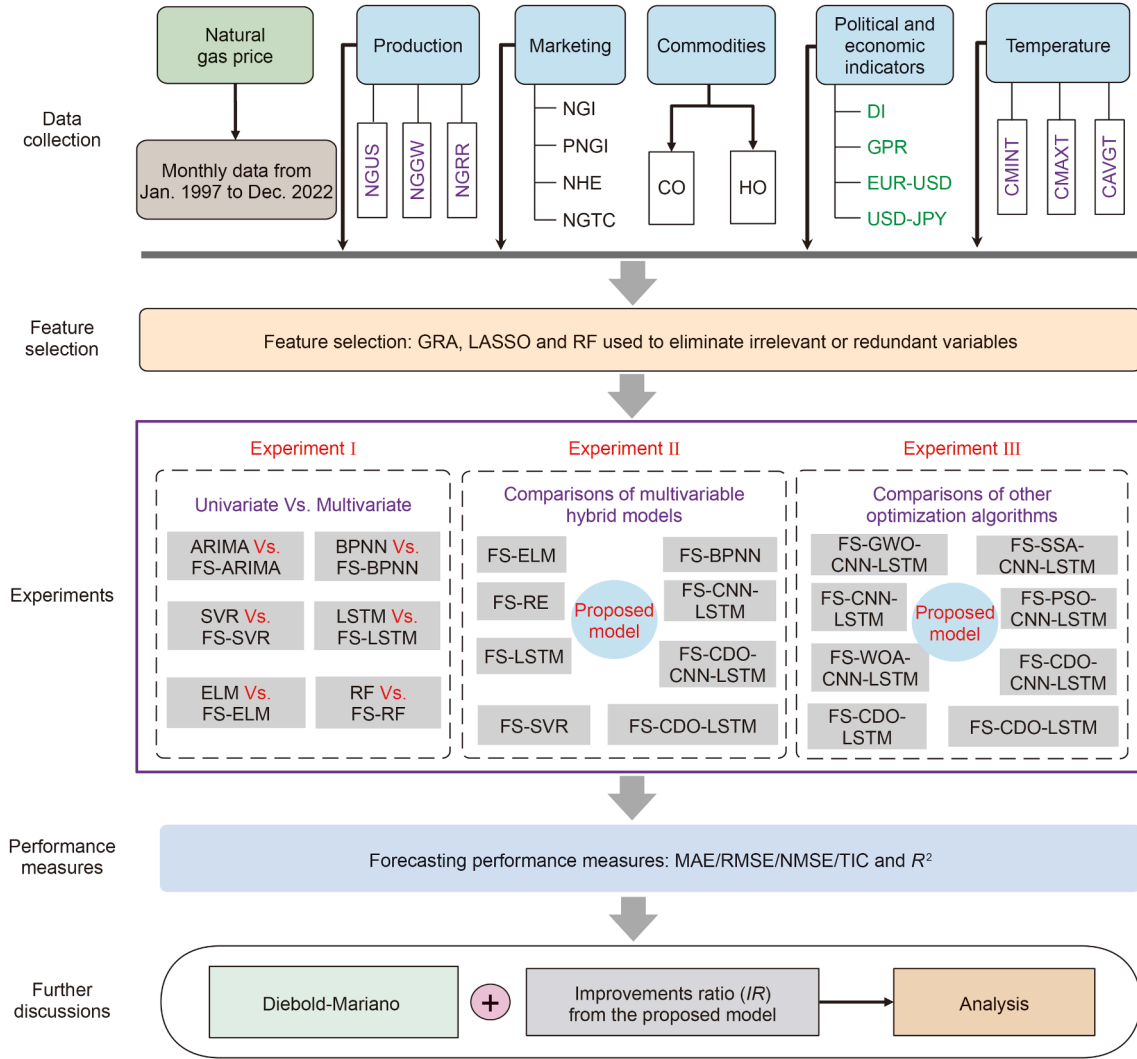


Fig. 1. The research framework of this study.

function serves to contract the original coefficients, causing the coefficients of unimportant variables to be diminished to zero. This effectively eliminates the impact of irrelevant variables on the model's predictive performance. The parameter is estimated using the following formula:

$$\hat{\beta}_{\text{Lasso}} = \underset{\beta}{\operatorname{argmin}} \left\| y - \sum_{i=1}^n x_i \beta_i \right\|^2 + \lambda \sum_{i=1}^n |\beta_i| \quad (1)$$

where the penalty parameter λ determines the model's complexity. As λ increases, the linear model's feature variables face a greater penalty. For further details on LASSO, refer to (Kapoor and Wichitakorn, 2023; Mishra et al., 2021; Tian et al., 2023).

3.1.2. Grey relation analysis (GRA)

GRA method is a method used to measure the degree of similarity or dissimilarity in the development trends between the target variable and its factors. The higher the correlation, the stronger the relationship with the target variable and the more significant the impact on the target variable. The detailed mathematical formulas are as follows (Guo et al., 2022; Liu and Yu, 2007).

$$\begin{cases} \theta_i = \frac{1}{n} \sum_{k=1}^n \zeta_i(k) \\ \zeta_i(k) = \frac{\min_j \min_l |x_0(l) - x_j(l)| + \gamma \max_j \max_l |x_0(l) - x_j(l)|}{|x_0(k) - x_i(k)| + \gamma \max_j \max_l |x_0(l) - x_j(l)|} \end{cases} \quad (2)$$

where θ_i represents the grey relation degree between the i -th factor and the target variable, and $\zeta_i(k)$ represents that of the i -th factor at the k -th moment. $\min_j \min_l |x_0(l) - x_j(l)|$ is the global minimum absolute difference between the target variable and all factors across all moments, and $\max_j \max_l |x_0(l) - x_j(l)|$ is the maximum. $\gamma \in [0, 1]$ represents recognition coefficient, generally set $\gamma = 0.5$.

3.1.3. Random forest (RF)

During feature selecting, RF uses bootstrap aggregating to build each decision tree (Breiman, 2001). Firstly, RF uses the Bootstrap sampling method to randomly draw samples from the original dataset. This process allows some samples to appear multiple

times in a single decision tree, while others may be excluded. For each decision tree's construction, RF randomly selects k features from the dataset as candidate features, limiting the splitting process to these k features. Typically, the value of k is set to the square root of the total number of features or a fraction of n , where n represents the total number of features.

RF algorithm has been successfully utilized for load forecasting (Fan et al., 2022), wave height forecasting (Ali et al., 2023), solar radiation energy (Prasad et al., 2019) and stock market forecasting (Park et al., 2022). Additionally, the detailed theoretical descriptions of RF can be found in the literature (Biau, 2012; Zhang et al., 2021; Behrens et al., 2018).

3.2. Chernobyl disaster optimizer (CDO)

The CDO algorithm (Shehadeh, 2023) is derived from the Chernobyl nuclear reactor core explosion. In this algorithm, nuclear explosions emit different kinds of radiation due to nuclear instability. The most common types of radiation include α , β and γ particles. CDO primarily concentrates on the updating methods of three types of particles. α , β and γ will pose a threat to humans. These particles will travel away from the reactor's core (a high-pressure area) towards regions where humans are located (low-pressure areas), ultimately leading to disaster. CDO assumes that the victims (humans) are moving as these particles attack them. Based on the estimation, the following equation simulates the process of speed decreasing to 0, where WS_h refers the walking speed of human (0–3 miles/h).

$$WS_h = 3 - 1 \times (3/\text{Maximum_Iteration}) \quad (3)$$

The gradient descent factors for the three particles when attacking humans is shown in Eq. (4).

$$\begin{cases} v_\gamma = (X_\gamma(t) - \rho_\gamma \cdot \Delta_\gamma) \\ v_\beta = 0.5 \times (X_\beta(t) - \rho_\beta \cdot \Delta_\beta) \\ v_\alpha = 0.25 \times (X_\alpha(t) - \rho_\alpha \cdot \Delta_\alpha) \end{cases} \quad (4)$$

where $X_i(t)$, $i = \gamma, \beta, \alpha$ represents the current position of gamma, beta and alpha particles; ρ_i , $i = \gamma, \beta, \alpha$ is the propagation of gamma, beta and alpha particles; Δ_i , $i = \gamma, \beta, \alpha$ is the difference between human positions and positions of gamma, beta and alpha particles.

By Eq. (5), the ρ_i , $i = \gamma, \beta, \alpha$ can be calculated.

$$\begin{cases} \rho_\gamma = \frac{X_h}{S_\gamma} - (WS_h \cdot \text{rand}()) \\ \rho_\beta = \frac{X_h}{0.5 \times S_\beta} - (WS_h \cdot \text{rand}()) \\ \rho_\alpha = \frac{X_h}{0.25 \times S_\alpha} - (WS_h \cdot \text{rand}()) \end{cases} \quad (5)$$

where X_h refers to the area in which humans are walking, represented as the area of a circle, which can be computed using Eq. (6). The speed of the particle, denoted as S_i , $i = \gamma, \beta, \alpha$, can randomly range from 1 to 300,000, with specific values such as 270,000 and 16,000 km/s, as shown in Table 1. To standardize this value, we apply the logarithmic transformation, as given in Eq. (6).

Table 1
Parameters of the CDO algorithm.

Radiation type	Speed of particle ($S_{\text{type of particle}}$), km/s
Alpha (α)	16,000
Beta (β)	270,000
Gamma (γ)	300,000

$$X_h = r^2 \cdot \pi \quad (6)$$

in which r is a random value within (0, 1).

$$\begin{cases} S_\gamma = \log(\text{rand}(1 : 300000)) \\ S_\beta = \log(\text{rand}(1 : 270000)) \\ S_\alpha = \log(\text{rand}(1 : 16000)) \end{cases} \quad (7)$$

The Δ_i , $i = \gamma, \beta, \alpha$ is the different from γ , β , α , and related positions are calculated using Eq. (8).

$$\Delta_i = |A_i \cdot X_i(t) - X_T(t)|, i = \gamma, \beta, \alpha \quad (8)$$

where $X_T(t)$ denotes the averages of whole positions, A_i , $i = \gamma, \beta, \alpha$ refers to the area over which these particles (γ , β , α), represented as the area of a circle, and is calculated using Eq. (9).

$$A_i = r^2 \cdot \pi, i = \gamma, \beta, \alpha \quad (9)$$

in which r is a random value within (0, 1).

On the basis of the Galileo Galilei equations of motion, the mean of total speed of γ , β and α can be taken through the following formula.

$$X_T = \frac{(v_\alpha \cdot v_\beta \cdot v_\gamma)}{3} \quad (10)$$

3.3. Forecasting models

The forecasting models employed in this study are described in detail as follows.

3.3.1. Long short-term memory (LSTM)

As a specialized form of recurrent neural network (RNN), LSTM (Hochreiter and Schmidhuber, 1997) can efficiently regulate information flow by introducing a gating mechanism, enabling it to better handle long-term dependencies. It stores and transmits information through unit states, which are designed to allow LSTM to retain long-term information without losing important details due to prolonged intervals. An LSTM unit consists of three gates: the input gate i_t , the forget gate f_t , and the output gate o_t .

Input gate:

$$i_t = \sigma(W_i[h_{t-1}, x_t] + b_i) \quad (11)$$

Forget gate:

$$f_t = \sigma(W_f[h_{t-1}, x_t] + b_f) \quad (12)$$

Output gate:

$$o_t = \sigma(W_o[h_{t-1}, x_t] + b_o) \quad (13)$$

Cell state:

$$\begin{cases} C_t = f_t \otimes C_{t-1} + i_t \otimes \tilde{C}_t \\ \tilde{C}_t = \tanh(W_C[h_{t-1}, x_t] + b_C) \end{cases} \quad (14)$$

Output vector:

$$h_t = o_t \otimes \tanh(C_t) \quad (15)$$

where x_t is input time series, \otimes represents the dot product; h_{t-1} denotes previous output; C_{t-1} , C_t and \tilde{C}_t are the previous memory state, current state and intermediate state, respectively.

3.3.2. Convolutional neural networks (CNN)

CNN is a type of deep feed-forward neural network that offers advantages like local connections and weight sharing, which has

achieved notable success in tasks. In this research, CNN is incorporated to boost the prediction accuracy of LSTM, using a one-dimensional convolution approach (Yao et al., 2023). And the related equations are shown as below.

$$Y = \sigma(\mathbf{W}^*X + b) \quad (16)$$

in which Y is the extracted features; \mathbf{W} is the weight matrix; X indicates the input data; b and ρ are bias vector and sigmoid function, respectively.

3.3.3. Support vector regression (SVR)

The core idea of SVR is to create a hyperplane in the feature space that maximizes the margin between the training data points and the hyperplane. To perform regression prediction, SVR introduces a notion of slack variables to allow for a certain degree of error tolerance. The goal of SVR is to reduce the complexity of the model while simultaneously reducing forecast inaccuracy and enlarging the margin (Chapelle et al., 1999).

Given training time series $\{(x_i, y_i)\}_{i=1}^n$, thereinto x_i is the input features, n denotes the length of the training time series and y_i represents the corresponding output value. The regression method can be built for the high-dimensional feature space expressed as following equation:

$$f(x) = \omega^* \Psi(x) + \nu \quad (17)$$

where $\Psi(x)$ represents the nonlinear mapping from the input space to the high-dimensional space, ω is the weight vector, and ν is the threshold value.

$$R(f) = \frac{1}{n} \sum_{i=1}^n L_\epsilon(y_i, f(x_i)) + \frac{1}{2} \|\omega\|^2 \quad (18)$$

where $L_\epsilon()$ represents loss function, C is the penalty parameter, ϵ represents tube size. Then Eq. (17) can be transformed into the following equation using two slack variables δ and δ^* :

$$\begin{aligned} \min & \frac{1}{2} \|\omega\|^2 + C \sum_{i=1}^n (\delta_i + \delta_i^*) \\ \text{s.t.} & \begin{cases} y_i - \omega_i^* \varphi(x_i) - b_i \leq \epsilon + \delta_i \\ \omega_i^* \varphi(x_i) + b - y_i \leq \epsilon + \delta_i^* \\ \delta_i + \delta_i^* \geq 0, i = 1, 2, \dots, n \end{cases} \end{aligned} \quad (19)$$

Thus, the dual form can be presented as the following equation:

$$\begin{aligned} \max & -\frac{1}{2} \sum_{i=1}^n \sum_{j=1}^n (\alpha_i - \alpha_i^*) (\alpha_j - \alpha_j^*) K(x_i, x_j) - \epsilon \sum_{i=1}^n (\alpha_i + \alpha_i^*) + \sum_{i=1}^n (\alpha_i - \alpha_i^*) \\ \text{s.t.} & \begin{cases} \sum_{i=1}^n (\alpha_i - \alpha_i^*) = 0 \\ 0 \leq \alpha_i \leq C, i = 1, 2, \dots, n \\ 0 \leq \alpha_i^* \leq C, i = 1, 2, \dots, n \end{cases} \end{aligned} \quad (20)$$

where α_i and α_i^* are Lagrange multipliers. $K(x_i, x_j) = \langle \varphi(x_i) \varphi(x_j) \rangle$ represents the kernel function, which can be written as:

$$K(x_i, x_j) = \exp\left(-\frac{\|x_i - x_j\|^2}{2\sigma}\right) = \exp(-\theta \|x_i - x_j\|^2) \quad (21)$$

where σ denotes the width of the radial basis function. The non-linear regression function is shown in Eq. (22).

$$f(x) = \sum_{i=1}^n (\alpha_i - \alpha_i^*) K(x_i, x_j) + b \quad (22)$$

3.4. The proposed combined model

Considering that both CNN-LSTM optimized by CDO algorithm (CDO-CNN-LSTM) and SVR perform well in the work, this study employs an adaptive weighting module (AWM), which can be used for parallel prediction using multiple models by assigning weight values to individual models, and ultimately constructs a more accurate prediction model. Firstly, the time series are inputted into the model, the results of CDO-CNN-LSTM and SVR can be obtained respectively, which are inputted into their respective thick layers and assigned different weight values by the AWM, and then the outputs of CDO-CNN-LSTM and SVR are linearly summed with the weights to construct the proposed combined model (CDO-CNN-LSTM&SVR). Finally, the forecasting values can be obtained using the following equation:

$$\hat{y} = \theta_1 \hat{y}_{M_1} + \theta_2 \hat{y}_{M_2} \quad (23)$$

where \hat{y}_{M_1} and \hat{y}_{M_2} are the forecasting values of CDO-CNN-LSTM and SVR, respectively. θ_1 , θ_2 are the corresponding weight matrices, \hat{y} is the output value of the added layer.

To dynamically evaluate model accuracy on sample data, AWM uses the following equation during the training process to find optimal weights:

$$APE = \left| \frac{\hat{y}_t - y_t}{y_t} \right| \quad (24)$$

APE indicates the absolute percentage error of the fitted and actual values, y_t and \hat{y}_t are the t -th observed and forecasting values, respectively. The combined model involves multiple stages, so it is necessary to analyze its complexity. The following is an asymptotic analysis of each stage of the combined model, which can be used as a reference for evaluating training time and hardware consumption.

Feature selection and CDO optimization: CDO for hyperparameter tuning operates with a complexity of $O(\text{Iterations} \times$

$\text{Population_Size} \times (O_{\text{SVR}} + O_{\text{LSTM}})$, where $O_{\text{LSTM}} \approx O(\text{num_epochs} \times \text{time_steps} \times \text{hidden_nodes}^2)$ and $O_{\text{SVR}} \approx O(n^3)$ (kernel matrix inversion) dominate the cost (Shi et al., 2024).

CNN-LSTM: Spatial-temporal modeling via Conv-Former and stacked LSTM introduces $O(L \times K \times Y \times \text{hidden_nodes}^2)$ operations per time step, where L, K, Y are the input length, kernel size, and output channels, respectively.

The asymptotic analysis reveals that the framework’s complexity aligns with the advanced hybrid models, e.g., variational mode decomposition (VMD)-PSO-deep belief network (DBN) (Li et al., 2021), FS-genetic algorithm (GA)-SVR (Zheng et al., 2023). Compared with the benchmark models in the experimental section of this study, such as ELM and BPNN, FS-CDO-CNN-LSTM&SVR still has an advantage in terms of complexity, where $O_{\text{ELM}} \approx O(L^3 + L^2 \times n)$ and $O_{\text{BPNN}} \approx O(\text{num_epochs} \times \text{time_steps} \times \text{hidden_nodes}^2)$. To further enhance real-time feasibility, lightweight strategies such as pruning redundant neurons (reducing hidden_nodes) or quantizing LSTM weights could be applied without sacrificing accuracy. Future work will integrate these optimizations and report empirical training times on edge devices.

4. Data description and feature selection

4.1. Influencing factors

This study selects the Henry Hub natural gas trading price, which has strong market liquidity and significant influence, as a case study to validate the effectiveness of the proposed model. Recent studies have consistently pointed out that highly correlated core influencing factors can help improve the prediction accuracy of energy prices (Wang et al., 2024; Zhang et al., 2025; Bao et al., 2025). However, natural gas prices are influenced by multiple factors, including supply and demand relationships, temperature changes, alternative energy prices (such as crude oil), and geopolitical risks (Zheng et al., 2023). Specifically, long-term trends in natural gas prices are driven by supply and demand, with natural gas inventory levels, production, imports and exports, and consumption having a significant impact on prices (Xing et al., 2024; Yarlagadda et al., 2024). Temperatures are also correlated with natural gas consumption, which indirectly affects natural gas prices (Li et al., 2022). The impact of the price linkage effect of alternative energy sources, such as crude oil as a core substitute, whose price volatility directly affects natural gas pricing (Perifanis and Dagoumas, 2021). Geopolitical risks, such as the Russia-Ukraine conflict, affect gas prices by triggering price volatility

through supply chain disruptions, export restrictions and investment uncertainty (Iliyasu et al., 2025). In addition, exchange rate fluctuations (e.g., EUR/USD, USD/JPY) can also have a non-linear impact on gas prices due to the cross-border nature of trading gas futures. Therefore, based on the above discussion and analysis, this study collects data on factors influencing natural gas prices from five dimensions: production, marketing, commodities, U.S. political and economic indicators, and temperature, as shown in Table 2. These data primarily originate from the U.S. Energy Information Administration (<https://www.eia.gov>) and the U.S. National Oceanic and Atmospheric Administration (<https://www.ncdc.noaa.gov>). Additionally, geopolitical risk index data is sourced from a website (<https://www.matteoiacoviello.com/gpr.htm>) (Caldara and Iacoviell, 2022). All data collected in this study are monthly data, spanning the period from January 1997 to December 2018, totaling 264 data points) is used as the training set, while the remaining 15% of the data (January 2019 to December 2022, totaling 48 data points) is regarded as the test set to validate the prediction model. In this study, the RobustScaler module in Scikit-learn is used to scale the data based on the median and the range of the upper (75%) and lower (25%) quartiles, in order to effectively deal with outliers. And the missing values are supplemented using linear interpolation. Additionally, the natural gas price series within the study period is tested for stationarity, and the Augmented Dickey-Fuller (ADF) test results indicate that the time series is a stationary series at the 5% significance level.

4.2. Feature selection (FS)

As shown in Table 2, there is a broad consensus that natural gas prices are affected by a multitude of factors, which renders the forecasting task a complicated procedure. Therefore, effective variable selection algorithms are essential for accurately predicting natural gas prices. Three widely used feature selection methods: LASSO, GRA and RF are introduced for variable screening, displayed in Table 3.

Specifically, these three methods are first used separately to conduct variable screening for natural gas price, with the related results presented in Table 4. Subsequently, the screened variables are compared and ranked. And then the common variables screened by at least two methods are identified as the important influencing factors, including NGRR, NGI and PNGI. Finally, these variables are utilized in subsequent model construction and forecasting tasks.

Table 2
Statistical characteristics of natural gas prices and related influencing variables.

Factor group	Variables	Acronym	Unit	Min	Max	Average	Std
Production	U.S. total natural gas Underground storage capacity	NGUS	MMcf	7,952,224	9,265,054	8688928.56	467400.23
	U.S. natural gas gross withdrawals	NGGW	MMcf	1,766,603	3,769,193	2450171.32	540029.48
	U.S. crude oil and natural gas rotary rigs in operation	NGRR	Count	250	2017	1161.55	480.39
Marketing	U.S. natural gas imports	NGI	MMcf	174,225	426,534	286141.02	54563.93
	Price of U.S. natural gas imports	PNGI	\$/MMcf	1.5	11.99	4.22	2.16
	U.S. natural gas exports	NHE	MMcf	9527	639,074	157629.60	162498.09
	U.S. natural gas total consumption	NGTC	MMcf	344,920	3,591,691	1931746.41	684581.85
Commodities	Cushing, OK crude oil future	CO	\$/Barrel	11.31	134.02	57.37	28.32
	Heating oil future	HO	\$/Gallon	0.312	4.30	1.74	0.91
Political and economic indicators of U.S.	US dollar index	DI	/	72.17	120.59	92.35	10.97
	Geopolitical risk index	GPR	/	0.95	10.85	2.77	1.16
	EUR/USD exchange rate	EUR-USD	/	0.85	1.5774	1.19	0.16
	USD/JPY exchange rate	USD-JPY	/	76.19	148.71	109.47	14.03
	Contiguous U.S. minimum temperature	CMINT	°F	−6.09	6.07	0.20	1.90
Temperature	Contiguous U.S. maximum temperature	CMAXT	°F	−6.04	7.60	0.30	2.21
	Contiguous U.S. average temperature	CAVGT	°F	−5.90	6.84	0.25	1.97

Table 3
Introductions of LASSO, GRA and RF methods.

Methods	Types of machine learning	Types of feature selection	Parameter values
LASSO	Supervised	Embedded	0.01 (penalty coefficient)
GRA	Unsupervised	Filter	0.5 (discrimination coefficient)
RF	Supervised	Embedded	100 (number of the estimators)

Table 4
Results of feature selection using LASSO, GRA and RF methods.

Methods	NGUS	NGGW	NGRR	NGI	PNGI	MHE	NGTC	CO
GRA	×	×	✓	✓	×	×	×	×
LASSO	×	×	✓	×	✓	×	✓	×
RF	×	×	✓	✓	✓	×	×	×
Rank	0	1	3	2	2	0	1	0
Methods	HO	DI	GPR	EUR-USD	USD-JPY	CMINT	CMAXT	CAVGT
GRA	×	✓	×	✓	✓	×	×	×
LASSO	✓	×	×	×	×	×	×	×
RF	×	×	✓	×	×	✓	×	×
Rank	1	1	1	1	1	1	0	0

5. Experiments and analysis

5.1. Performance measures

Six widely recognized metrics are used to evaluate the forecasting performance of both the developed and comparison models, including mean absolute error (MAE), root mean square error (RMSE), normalized mean square error (NMSE), Theil inequality coefficient (TIC) and coefficient of determination (R^2):

$$MAE = \frac{1}{T} \sum_{t=1}^T |y_t - \hat{y}_t| \quad (26)$$

$$RMSE = \sqrt{\frac{1}{T} \sum_{t=1}^T (y_t - \hat{y}_t)^2} \quad (27)$$

$$NMSE = \frac{1}{T} \sum_{t=1}^T \frac{(y_t - \hat{y}_t)^2}{y_t \cdot \hat{y}_t} \quad (28)$$

$$TIC = \frac{\sqrt{\frac{1}{T} \sum_{t=1}^T (y_t - \hat{y}_t)^2}}{\sqrt{\frac{1}{T} \sum_{t=1}^T y_t^2} + \sqrt{\frac{1}{T} \sum_{t=1}^T \hat{y}_t^2}} \quad (29)$$

$$R^2 = 1 - \frac{\sum_{t=1}^T (\hat{y}_t - y_t)^2}{\sum_{t=1}^T (y_t - \bar{y})^2} \quad (30)$$

where y_t denotes the t -th actual value, \hat{y}_t means the t -th predicted value, and \bar{y} is the average value of the data.

5.2. Experimental design

Three experiments are conducted to evaluate the prediction performance of both the comparison models and the proposed FS-CDO-CNN-LSTM&SVR model, providing a comprehensive

assessment of the model's forecasting effectiveness. Specifically, Experiment I focuses on highlighting the benefits of the multivariate model by comparing it with the univariate model. Immediately after that, based on the high-performance multivariate prediction models identified in Experiment I, Experiment II is firstly used to select the optimal single model through comparison. It then validates the superiority of the benchmark model by contrasting it with the improved optimal single model. Finally, it comprehensively compares and analyzes the advantages of the designed FS-CDO-CNN-LSTM & SVR model with regard to improving the forecasting effectiveness. Additionally, Experiment III is designed to further compare and analyze the optimization algorithm, CNN and the proposed combined model to highlight the advantages of the proposed model. More details are presented in the subsequent subsections.

5.3. Experiment I: can multivariate prediction improve prediction accuracy?

Experiment I is designed to test whether multivariate prediction can improve the prediction accuracy by comparing univariate and multivariate models, and to demonstrate the prediction effect of combined variable screening models. It also introduces six single forecasting models commonly used in energy prices prediction, including LSTM, BPNN, ELM, ARIMA, RF and SVR, and utilizes these methods to compare them with their multivariate versions by using FS methods. The forecasting errors of forecasting models in Experiment I are presented in Table 5 and Fig. 2. Based

Table 5
Forecasting errors of forecasting models with univariate and multivariate variables.

Variables	Models	MAE	RMSE	NMSE	TIC	R^2
Univariate	RF	0.8310	1.1378	0.3414	0.1409	0.6586
	BPNN	0.6805	1.0743	0.3101	0.1287	0.6899
	ARIMA	0.7375	1.0470	0.2945	0.1306	0.7055
	ELM	0.7039	1.0229	0.2812	0.1235	0.7188
	SVR	0.6967	1.0373	0.2891	0.1236	0.7109
	LSTM	0.6930	1.0215	0.2804	0.1221	0.7196
Multivariate	FS-RF	0.5919	0.9319	0.2334	0.1107	0.7666
	FS-BPNN	0.5695	0.8391	0.1892	0.1018	0.8108
	FS-ARIMAX	0.7879	1.0897	0.3191	0.1409	0.6809
	FS-ELM	0.6942	0.9210	0.2279	0.1109	0.7721
	FS-SVR	0.5541	0.7683	0.1586	0.0919	0.8414
	FS-LSTM	0.5330	0.8187	0.1801	0.1008	0.8199

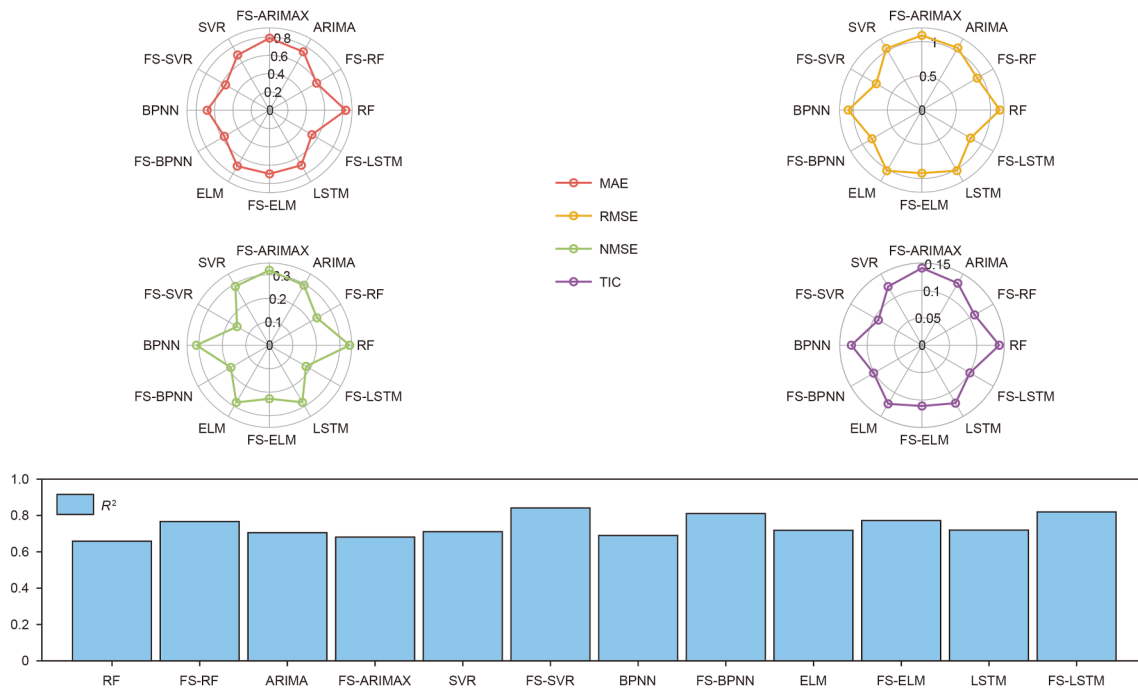


Fig. 2. Performance measures of univariate and multivariate forecasting models.

on the results of Table 5 and Fig. 2, the related analysis and discussions can be centered on the following three aspects:

- (1) In the comparison of six univariate benchmark models, LSTM and SVR are noted for demonstrating superior prediction levels in natural gas price forecasting. As the results presented in Table 5, both LSTM and SVR outperform other single models in terms of multiple evaluation metrics. For instance, LSTM achieves a MAE of 0.6930 and an R^2 of 0.7196, while SVR attains a MAE of 0.6967 and an R^2 of 0.7109. These results emphasize the effectiveness of machine learning methods, especially LSTM and SVR, in energy price modeling and forecasting.
- (2) These six single models with multivariate variables using feature selection are also tested in this experiment. As shown in Table 5, the FS-ARIMAX model performs poorly, struggling to match the predictive capabilities of the neural network model with multivariate inputs. Specifically, FS-ARIMAX has a significantly higher NMSE of 0.3191 and a lower R^2 of 0.6809 than ARIMA. This further indicates that the classical statistical model ARIMA may fail to effectively utilize the multivariate characteristics of the dataset. Conversely, feature-selection-based multivariate AI models demonstrate superior predictive performance, with R^2 values of 0.8199, 0.8414 and 0.8108 for FS-LSTM, FS-SVR and FS-BPNN, respectively.
- (3) An important finding of this experiment is that under identical model architectures, multivariate models demonstrate superior predictive performance compared to univariate models. The multivariate models represented by FS-LSTM, FS-SVR and FS-BPNN consistently outperform their corresponding univariate ones. For example, the R^2 values of FS-LSTM, FS-SVR, and FS-BPNN are 0.8199, 0.8414, and 0.8108, respectively, considerably bigger than those of the corresponding univariate models. It indicates that multivariate models can significantly enhance the forecasting accuracy, except for the FS-ARIMAX model. The lower MAE and RMSE

values of FS-LSTM and FS-SVR further emphasize the superiority of multivariate models.

In summary, this experiment demonstrates that multivariate models, especially those utilizing AI techniques such as LSTM and SVR, can significantly outperform univariate models in natural gas price forecasting. In addition, this experiment also emphasizes the importance of effective feature selection and points out the limitations of the ARIMA model in enhancing predictive capabilities within multivariate contexts. These findings mentioned above highlight the potential of multivariate AI forecasting methods to enhance the prediction accuracy of natural gas price. This improvement may be attributed to the ability of these models to more effectively capture the relationship between input features and the target series, thereby boosting their predictive performance.

5.4. Experiment II: comparisons of multivariate hybrid models

According to the results of Experiment I, the predictive capacity of multivariate models is typically superior to univariate models. Therefore, Experiment II is designed to compare the multivariate models and then select the models with the best prediction effect, i.e., SVR and LSTM. Then this study attempts to improve these two models, particularly the LSTM model. By introducing the CNN layer to connect with the LSTM model, the model can realize the deep mining of the correlation between input features. In addition, intelligent optimization algorithms are also introduced to help find the most suitable model parameters. Finally, these models are compared with the proposed hybrid model FS-CDO-CNN-LSTM&SVR. The results demonstrate that this model achieves a significant improvement in prediction performance compared to previous models. Moreover, Table 6 and Fig. 3 give the prediction results of different models, where several discussions can be analyzed as below.

- (1) Among the FS-ELM, FS-RF, FS-LSTM, FS-SVR and FS-BPNN, the MAE value of FS-LSTM is 0.5330, better than the other

Table 6
Forecasting errors of the proposed model and the comparison models.

Models	MAE	RMSE	NMSE	TIC	R^2
FS-ELM	0.6942	0.9210	0.2279	0.1109	0.7721
FS-RF	0.5919	0.9319	0.2334	0.1107	0.7666
FS-LSTM	0.5330	0.8187	0.1801	0.1008	0.8199
FS-SVR	0.5541	0.7683	0.1586	0.0919	0.8414
FS-BPNN	0.5695	0.8391	0.1892	0.1018	0.8108
FS-CNN-LSTM	0.5681	0.7983	0.1712	0.1006	0.8288
FS-CDO-CNN-LSTM	0.5057	0.7222	0.1401	0.0905	0.8599
FS-CDO-LSTM	0.4948	0.7438	0.1487	0.0928	0.8513
FS-CDO-CNN-LSTM&SVR	0.3580	0.6029	0.0977	0.0730	0.9023

- models. And the R^2 value of FS-LSTM is 0.8199, just lower than 0.8414 of FS-SVR. For RMSE, NMSE and NMSE, FS-SVR has the smallest values. Consequently, it can be concluded that among the five improved multivariate AI models, SVR has the best prediction performance, followed by LSTM. Meanwhile, these two models are the most commonly used models in natural gas price prediction, which is corroborated by the results of this experiment.
- (2) The MAE value of FS-CNN-LSTM is 0.5681, higher than that of FS-LSTM. For the remaining measures, FS-CNN-LSTM consistently outperforms FS-LSTM, indicating that the CNN layer can improve the performance of LSTM. In addition, the NMSE and R^2 values of FS-CDO-LSTM are 0.1487 and 0.8513, significantly outperforming FS-LSTM. The superior prediction results achieved by FS-CNN-LSTM stem precisely from its integration of the strengths of both the convolutional neural network and the long short-term memory network.
- (3) Finally, through comparisons between FS-CDO-CNN-LSTM&SVR and the benchmark models, it is evident that the

forecasting effectiveness of the proposed model has witnessed a significant boost. For instance, the NMSE value of FS-CDO-CNN-LSTM&SVR is 0.0977, nearly half of the NMSE value of FS-LSTM. And its R^2 value is 0.9023, which exceeds the results achieved by the other forecasting models. In conclusion, the aforementioned comparisons show that the proposed combined model can effectively enhance the forecasting accuracy of natural gas price by combining FS, CNN-LSTM, CDO and SVR technologies.

5.5. Experiment III: comparisons of other optimization algorithms

The primary objective of Experiment III is to investigate the effectiveness of different optimization algorithms. A variety of commonly used algorithms, including grey wolf optimization (GWO), sparrow search algorithm (SSA), particle swarm optimization (PSO), whale optimization algorithm (WOA), and the newly proposed CDO, are applied in this study to combine with the FS-CNN-LSTM model. In addition, Experiment III also covers the investigation of the effect of CNN on the amplification of LSTM model. Finally, this experiment conducts a comprehensive comparative analysis between the proposed combined model and all enhancement models. Additionally, the forecasting results of the proposed model and benchmark models are presented in Table 7 and Fig. 4. Through comparing the results across different models, the following conclusions can be drawn:

- (1) Enhancements of the optimization algorithm: The adoption of optimization algorithms significantly enhances the prediction performance of the FS-CNN-LSTM model. Models employing optimization algorithms, including FS-CNN-GWO-LSTM, FS-CNN-SSA-LSTM, FS-CNN-PSO-LSTM, FS-

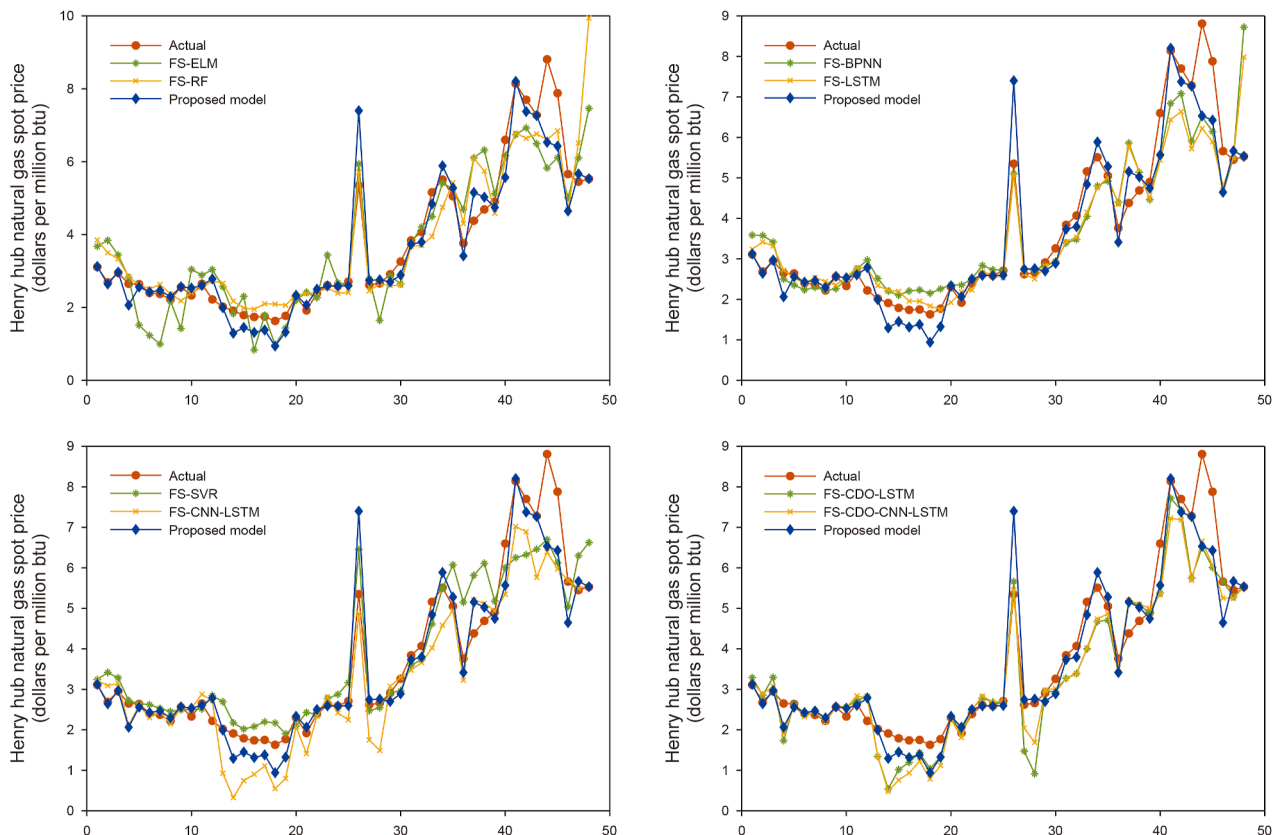


Fig. 3. Forecasting results of the comparison models and proposed forecasting model.

Table 7
Forecasting errors of forecasting models with different optimization algorithms.

Models	MAE	RMSE	NMSE	TIC	R^2
FS-CNN-LSTM	0.5681	0.7983	0.1712	0.1006	0.8288
FS-CDO-LSTM	0.4948	0.7438	0.1487	0.0928	0.8513
FS-PSO-CNN-LSTM	0.5889	0.7780	0.1626	0.0972	0.8374
FS-WOA-CNN-LSTM	0.5501	0.7636	0.1567	0.0950	0.8433
FS-SSA-CNN-LSTM	0.5452	0.7574	0.1541	0.0946	0.8459
FS-GWO-CNN-LSTM	0.5282	0.7416	0.1478	0.0922	0.8522
FS-CDO-CNN-LSTM	0.5057	0.7222	0.1401	0.0905	0.8599
FS-CDO-CNN-LSTM&SVR	0.3580	0.6029	0.0977	0.0730	0.9023

CNN-WOA-LSTM and FS-CNN-CDO-LSTM, consistently outperform the baseline FS-CNN-LSTM model with regard to MAE, RMSE, NMSE, TIC, and R^2 .

- (2) The superiority of CDO algorithm over other optimization algorithms: The results listed in Table 7 indicate that CDO algorithm exhibits the most substantial improvement in predictive accuracy when compared to other optimization algorithms. The proposed FS-CNN-CDO-LSTM model outperforms all other algorithm-enhanced models in terms of all the performance measures, achieving impressive results with a MAE of 0.5057 and an R^2 of 0.8599. This fully highlights the exceptional effectiveness of CDO in optimizing the FS-CNN-LSTM framework.

- (3) Impacts of CNN on LSTM: It is evident that integrating CNN with LSTM models can lead to a noticeable improvement in prediction performance. Compared with similar models, the LSTM model incorporating CNN can obtain lower MAE, RMSE, NMSE values and higher R^2 values, which suggests that the predictive capability of LSTM can be effectively enhanced by applying CNN.
- (4) The superiority of the constructed FS-CDO-CNN-LSTM&SVR model: the proposed model demonstrates optimal performance among all prediction models, achieving the lowest MAE value (0.3580) and the highest R^2 value (0.9023). This developed model demonstrates the predictive power of combining feature selection, CDO, CNN, LSTM and SVR to create a comprehensive and highly accurate predictive framework for energy prices, such as natural gas price.

In conclusion, Experiment III showcases the substantial effect of optimization algorithms, particularly CDO, in terms of improving forecasting accuracy of the FS-CNN-LSTM. Furthermore, the addition of CNN layer enhances the performance of LSTM. Finally, the FS-CDO-CNN-LSTM & SVR model developed in this study significantly outperforms the comparison methods. These findings highlight the potential of utilizing optimization algorithms, CNN, and combined strategy for improving the prediction accuracy of natural gas price.

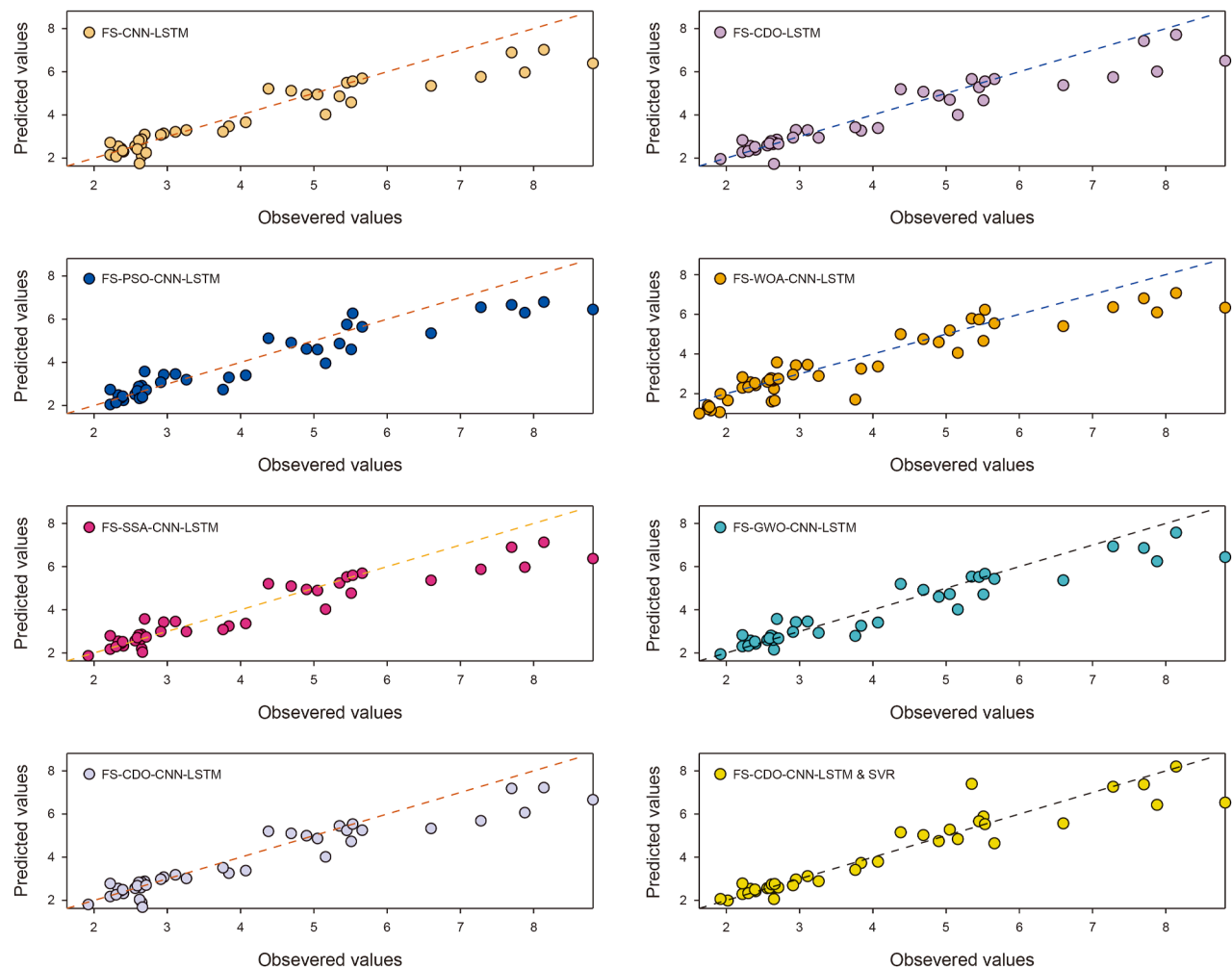


Fig. 4. Forecasting results of the forecasting models with other optimization algorithms.

6. Further discussions

In this section, the Diebold-Mariano (DM) test, forecasting effectiveness, the improvements ratio (IR) from the proposed model compared with benchmark models, and additional cases for crude oil price forecasting are discussed in this work.

6.1. Hypothesis testing

In this subsection, DM test (Diebold and Mariano, 1995), a well-established statistical hypothesis testing in time series prediction, is adopted to evaluate whether there are significant differences in forecasting performance between the proposed method and each of the benchmark models. Additionally, to further validate the prediction performance, both the forecasting effectiveness (Xiao et al., 2016; Xing et al., 2024) and the variance of forecasting errors (Var_{error}) are calculated, demonstrating the superiority of the developed combined model over the other models. The detailed results are shown in Table 8.

- (1) Hypothesis testing is conducted to ascertain if there is a remarkable difference in forecasting performance between the proposed model and the comparison model at a given significance level. From the results presented in Table 8, it is evident that when comparing the proposed model with the univariate model, their DM test values are consistently higher than $Z_{0.10/2} = 1.65$, indicating that significant difference of the prediction performance between the developed model and the univariate model under $\alpha = 0.10$. When comparing with the other multivariate models, it is found that the DM test values are higher than $Z_{0.15/2} = 1.44$ in the vast majority of cases, and more than half of the cases are higher than $Z_{0.10/2} = 1.65$, showing a noticeable difference in forecasting performance when the proposed method is compared with the other benchmark models. Furthermore, based on the experimental results presented in Section 5, it is evident that the combined model in this study achieves highly accurate natural gas price predictions.
- (2) The forecasting effectiveness of the models is used to compare the accuracy of the proposed combined model and other nineteen benchmark models. A higher predictive validity score indicates better predictive performance of the

model. As shown in Table 8, the forecasting effectiveness values of the univariate models are lower than those of the multivariate models. While there are variations in the forecasting effectiveness across the different models, the proposed combined model consistently achieves the highest value. This suggests that the proposed model offers superior predictive accuracy and outperforms all other comparative models.

- (3) The robustness of the model's forecasting performance is assessed by introducing the variance of forecasting errors. According to the results in Table 8, the variance of prediction errors for the univariate model is relatively larger, exceeding 1.0. In contrast, the multivariate model exhibits a smaller variance, although there is a noticeable difference in error variance between different models. Overall, the proposed method shows the smallest error variance of 0.3547, indicating that it possesses the optimal predictive robustness and stability among the twenty models.

6.2. Improvement ratio (IR) of the proposed model compared to comparison models

The improvement rate (IR) (Xing et al., 2022) metric is constructed to determine whether the proposed model has improved in terms of prediction accuracy compared to the other models.

$$IR_{Index} = \left| \frac{Index_{comparison} - Index_{proposed}}{Index_{comparison}} \right| \times 100\% \quad (31)$$

where IR_{Index} is an improvement ratio from the proposed model compared to the benchmark methods, $Index$ represents the model performance measure, including the MAE, RMSE, NMSE, TIC and R^2 .

Within this subsection, the effectiveness of the proposed combined forecasting model is evaluated by means of comparing it with several benchmark models, including RF, SVR, LSTM, ELM, ARIMA, and BPNN. The evaluation is based on the improvement ratio across five model performance metrics. The IR results of the proposed model relative to the benchmark model are presented in Table 9. From these results, it is evident that the developed model significantly outperforms the benchmark models in forecasting performance. The more detailed analysis is provided as below.

- (1) Although the prediction performance of each univariate model varies, the IR values presented in Table 9 are consistently high across all models, such as IR_{NMSE} values greater than 65%. This not only reflects the superior forecasting effectiveness of the proposed model compared with the univariate model, but also points out the deficiency of the univariate forecasting methods in predicting natural gas price without considering the data of influencing factors. It further indicates that future research should pay more attention to the innovation of introducing multivariate data and multivariate models.
- (2) For multivariate models, the IR values in Table 9 are generally lower than those of corresponding univariate models, reflecting that multivariate comparison models outperform univariate comparison methods in predictive performance. For instance, the IR_{R^2} values of the developed model with respect to RF and FS-RF are 37.0027% and 17.7015%, respectively. In addition, compared to single models and their multivariate versions, hybrid models considering CNN layer and optimization algorithms exhibit lower IR values. This

Table 8
Results for the DM test and the forecasting effectiveness of forecasting models.

Variables	Models	DM test	FE-1	FE-2	Var_{error}
Univariate	RF	−1.8424	0.8258	0.6981	1.0914
	SVR	−1.6916	0.8186	0.6921	1.0932
	LSTM	−1.7590	0.8202	0.6971	1.0626
	ELM	−1.6584	0.8169	0.6763	1.0608
	ARIMA	−2.9310	0.8221	0.7262	1.0817
	BPNN	−1.6030	0.8347	0.7049	1.1785
Multivariate	FS-RF	−1.1860	0.8523	0.7404	0.8831
	FS-SVR	−1.7271	0.8592	0.7720	0.5956
	FS-LSTM	−1.6772	0.8766	0.7937	0.6662
	FS-ELM	−2.8416	0.7985	0.6698	0.8606
	FS-ARIMAX	−3.2522	0.8181	0.7369	0.9276
	FS-BPNN	−1.4148	0.8534	0.7542	0.7181
	FS-CDO-LSTM	−1.4410	0.8487	0.7077	0.4441
	FS-CDO-CNN-LSTM	−1.2950	0.8448	0.7034	0.3922
	FS-CNN-LSTM	−2.1727	0.8161	0.6569	0.4610
	FS-PSO-CNN-LSTM	−2.0508	0.8165	0.6561	0.4779
	FS-SSA-CNN-LSTM	−1.7441	0.8359	0.6987	0.4656
	FS-GWO-CNN-LSTM	−1.3866	0.8428	0.7077	0.4554
	FS-WOA-CNN-LSTM	−1.6022	0.8471	0.7350	0.4992
	FS-CDO-CNN-LSTM&SVR	−	0.9014	0.8043	0.3547

Table 9
The improvement ratio of the proposed model compared to the comparison models.

Variables	Models	$IR_{MAE}, \%$	$IR_{RMSE}, \%$	$IR_{NMSE}, \%$	$IR_{TIC}, \%$	$IR_{R^2}, \%$
Univariate	RF	56.9194	47.0118	71.3825	48.1902	37.0027
	SVR	48.6149	41.8780	66.2055	40.9385	26.9236
	LSTM	48.3405	40.9790	65.1569	40.2129	25.3891
	ELM	49.1405	41.0597	65.2560	40.8907	25.5287
	ARIMA	51.4576	42.4164	66.8251	44.1041	27.8951
Multivariate	BPNN	47.3916	43.8797	68.4940	43.2789	30.7871
	FS-RF	39.5168	35.3042	58.1405	34.0560	17.7015
	FS-SVR	35.3907	21.5280	38.3985	20.5658	7.2379
	FS-LSTM	32.8330	26.3589	45.7524	27.5794	10.0500
	FS-ELM	48.4298	34.5385	57.1303	34.1749	16.8631
	FS-ARIMAX	54.5628	44.6728	69.3826	48.1902	32.5158
	FS-BPNN	37.1378	28.1492	48.3615	28.2908	11.2852
	FS-CDO-LSTM	27.6475	18.9433	34.2972	21.3362	5.9908
	FS-CDO-CNN-LSTM	29.2070	16.5190	30.2641	19.3370	4.9308
	FS-CNN-LSTM	36.9829	24.4770	42.9322	27.4354	8.8682
	FS-PSO-CNN-LSTM	39.2087	22.5064	39.9139	24.8971	7.7502
	FS-SSA-CNN-LSTM	34.3360	20.3987	36.5996	22.8330	6.6675
	FS-GWO-CNN-LSTM	32.2226	18.7028	33.8972	20.8243	5.8789
	FS-WOA-CNN-LSTM	34.9209	21.0450	37.6516	23.1579	6.9963

not only highlights the limitations of single models but also underscores the advantage of hybrid models, further validating the scientific credibility and effectiveness of the proposed forecasting model.

In comprehensive comparisons, regardless of univariate or multivariate models, the corresponding IR_{MAE} , IR_{RMSE} , IR_{NMSE} and IR_{TIC} values of the proposed model are basically greater than 20%, and the corresponding IR_{R^2} values are greater than 5%, revealing the superior predictive performance of the presented combined forecasting approach. Based on the experimental results and discussions in Section 5, along with the IR analysis in this section, it is evident that the proposed model outperforms the nineteen comparison models in terms of prediction accuracy.

6.3. Robustness test

To further validate the generalizability of the proposed model, this subsection introduces monthly WTI crude oil price dataset from January 2000 to December 2022 for validation. Based on the relevant references (Xu et al., 2025; Jin and Xu, 2024), the three core influencing factor variables of silver price, EUR/USD, and Henry Hub natural gas price are screened out. Table 10 shows the prediction results of different models on the WTI crude oil dataset. From the results in Table 10, it can be seen that the proposed FS-CDO-CNN-LSTM&SVR model performs best on the WTI crude oil dataset, with the lowest MAE (5.8096), lowest (RMSE (7.8838), lowest NMSE (0.1139), TIC (0.0572), and highest R^2 (0.8879). This indicates that the proposed model can effectively capture the complex patterns of WTI crude oil price fluctuations, demonstrating strong generalization ability. Notably, models using

Table 10
Forecasting errors of the proposed model and comparison models for WTI crude oil price.

Models	MAE	RMSE	NMSE	TIC	R^2
FS-CNN-LSTM	8.4122	10.5350	0.2014	0.0742	0.7986
FS-CDO-LSTM	7.9481	10.1983	0.1894	0.0757	0.8113
FS-PSO-CNN-LSTM	7.8230	9.7172	0.1713	0.0726	0.8287
FS-WOA-CNN-LSTM	7.2418	9.1379	0.1515	0.0681	0.8485
FS-SSA-CNN-LSTM	6.5393	8.6473	0.1357	0.0631	0.8643
FS-GWO-CNN-LSTM	6.8332	9.0145	0.1475	0.0645	0.8525
FS-CDO-CNN-LSTM	6.2163	8.3982	0.1283	0.0615	0.8721
FS-CDO-CNN-LSTM&SVR	5.8096	7.8838	0.1139	0.0572	0.8879

ensemble optimization algorithms such as SSA, WOA, and CDO consistently outperform the baseline FS-CNN-LSTM model, suggesting that these algorithms enhance the predictive performance of the model. The TIC values, which measure the extent of prediction bias relative to actual data, also confirm the stability of models using optimization algorithms. The relatively high R^2 values also indicate that the proposed model possesses strong explanatory power, even when applied to different energy commodities. This robustness may stem from the feature selection (FS) mechanism and the hybrid architecture's ability to effectively capture the nonlinear characteristics of energy prices. In summary, the stable performance across different energy datasets confirms the robustness of the proposed framework, providing a reference for other energy price market predictions.

7. Conclusions

Natural gas plays a crucial role in the global energy market and is increasingly becoming a primary energy source for many nations due to its relatively low-carbon footprint. As global natural gas trade expands, its price forecasting has become essential for macroeconomic decision-making, portfolio administration, and risk control. Nevertheless, influenced by multiple factors such as supply-demand dynamics, exchange rate fluctuations, macroeconomic policies, extreme weather, conflicts, and environmental factors, natural gas price exhibits non-stationarity, non-linearity and complexity characteristics, making accurately forecasting natural gas price a challenging task.

To achieve extremely precise and reliable prediction results, this study develops a combined model for natural gas price prediction, which integrates feature selection, intelligent optimization approaches, and machine learning technologies. Furthermore, to validate the performance of the proposed model, comprehensive experimental comparisons and analyses are carried out using monthly natural gas trading price data from the Henry Hub in the United States as a case study. In addition, with the aim of further verifying the effectiveness and generalization ability of the FS-CDO-CNN-LSTM&SVR model, the discussion section comprehensively evaluates its predictive performance through hypothesis testing, forecasting effectiveness, and improvement ratio. Through the experimental comparisons and discussions, it can be found that compared with the other forecasting models discussed in this study, the proposed model demonstrates outstanding forecasting

capabilities in natural gas price prediction and significantly improves prediction accuracy. Specifically, on the one hand, compared to single models with univariate inputs, single models that consider multiple factors exhibit higher prediction accuracy, showing the importance of multivariate data in improving the performance of natural gas price prediction. On the other hand, optimization algorithms and CNNs can significantly improve the prediction performance of standalone LSTM models. By integrating optimization techniques and CNN layers into hybrid LSTM models, the limitations of standalone LSTM models can be addressed, thereby achieving enhanced predictive accuracy. Ultimately, the proposed combined model outperforms other hybrid models in natural gas price forecasting. This superiority and robustness are further confirmed through hypothesis testing, forecasting effectiveness analysis, and improvement ratio assessments.

In summary, the developed combined forecasting model for natural gas price demonstrates both high prediction accuracy and robustness, while also serving as a valuable reference for time series forecasting in other energy price domains. In future research, we will conduct in-depth studies on energy price forecasting and actively incorporate cutting-edge forecasting techniques to further enhance prediction accuracy.

CRediT authorship contribution statement

Pei Du: Writing – review & editing, Writing – original draft, Software, Investigation, Conceptualization. **Xuan-Kai Zhang:** Writing – original draft, Visualization, Software, Data curation. **Jun-Tao Du:** Writing – review & editing, Validation, Supervision, Project administration. **Jian-Zhou Wang:** Writing – review & editing, Supervision, Formal analysis.

Declaration of competing interest

The authors declare that they have no known competing financial interests or personal relationships that could have appeared to influence the work reported in this paper.

Acknowledgments

This study was supported by the funding from the Humanities and Social Science Fund of Ministry of Education of China (No. 22YJZ028), National Natural Science Foundation of China (Grant No. 72303001), Fundamental Research Funds for the Central Universities (No. JUSRP124043), Anhui Provincial Excellent Young Scientists Fund for Universities (No. 2024AH030001), Anhui Education Department Excellent Young Teachers Fund (No. YQYB2024021) and Basic Research Program of Jiangsu (No. BK20251593).

References

- Ali, M., Prasad, R., Xiang, Y., Jamei, M., Yaseen, Z.M., 2023. Ensemble robust local mean decomposition integrated with random forest for short-term significant wave height forecasting. *Renew. Energy* 205, 731–746. <https://doi.org/10.1016/j.renene.2023.01.108>.
- Bao, H., Hong, Y., Sun, Y., Wang, S., 2025. A novel hybrid nonlinear forecasting model for interval-valued gas prices. *J. Forecast.* 44 (5), 1826–1848. <https://doi.org/10.1002/for.3272>.
- Behrens, C., Pierdzioch, C., Risse, M., 2018. Testing the optimality of inflation forecasts under flexible loss with random forests. *Econ. Modell.* 72, 270–277. <https://doi.org/10.1016/j.econmod.2018.02.004>.
- Biau, G., 2012. Analysis of a random forests model. *J. Mach. Learn. Res.* 13, 1063–1095. <https://dl.acm.org/doi/10.5555/2188385.2343682>.
- Breiman, L., 2001. Random forests. *Mach. Learn.* 45, 5–32. <https://doi.org/10.1023/A:1010933404324>.
- Cabelló-López, T., Carranza-García, M., Riquelme, J.C., García-Gutiérrez, J., 2023. Forecasting solar energy production in Spain: a comparison of univariate and

- multivariate models at the national level. *Appl. Energy* 350, 121645. <https://doi.org/10.1016/j.apenergy.2023.121645>.
- Caldara, D., Iacoviell, M., 2022. Measuring geopolitical risk. *Am. Econ. Rev.* 112 (4), 1194–1225. <https://doi.org/10.1257/aer.20191823>.
- Čeperić, E., Žiković, S., Čeperić, V., 2017. Short-term forecasting of natural gas prices using machine learning and feature selection algorithms. *Energy* 140, 893–900. <https://doi.org/10.1016/j.energy.2017.09.026>.
- Chapelle, O., Haffner, P., Vapnik, V.N., 1999. Support vector machines for histogram-based image classification. *IEEE Trans. Neural Network.* 10, 1055–1064. <https://doi.org/10.1109/72.788646>.
- Diebold, F.X., Mariano, R.S., 1995. Comparing predictive accuracy. *J. Bus. Econ. Stat.* 13, 253–263. <https://doi.org/10.1080/07350015.1995.10524599>.
- Du, P., Wang, J., Yang, W., Niu, T., 2018. Multi-step ahead forecasting in electrical power system using a hybrid forecasting system. *Renew. Energy* 122, 533–550. <https://doi.org/10.1016/j.renene.2018.01.113>.
- Ervural, B.C., Beyca, O.F., Zaim, S., 2016. Model estimation of ARMA using genetic algorithms: a case study of forecasting natural gas consumption. *Proc. Soc. Behav. Sci.* 235, 537–545. <https://doi.org/10.1016/j.sbspro.2016.11.066>.
- Fan, G.F., Zhang, L.Z., Yu, M., Hong, W.C., Dong, S.Q., 2022. Applications of random forest in multivariable response surface for short-term load forecasting. *Int. J. Electr. Power Energy Syst.* 139, 108073. <https://doi.org/10.1016/j.ijepes.2022.108073>.
- Gao, Y., Li, P., Yang, H., Wang, J., 2023. A solar radiation intelligent forecasting framework based on feature selection and multivariable fuzzy time series. *Eng. Appl. Artif. Intell.* 126 (C), 106986. <https://doi.org/10.1016/j.engappai.2023.106986>.
- Guan, R., Wang, A., Liang, Y., Fu, J., Han, X., 2022. International natural gas price trends prediction with historical prices and related news. *Energies* 15 (10), 3573. <https://doi.org/10.3390/en15103573>.
- Guo, Z.H., Wu, J., Lu, H.Y., Wang, J.Z., 2011. A case study on a hybrid wind speed forecasting method using BP neural network. *Knowl. Base Syst.* 24 (7), 1048–1056. <https://doi.org/10.1016/j.knosys.2011.04.019>.
- Guo, A., Kong, D., Zhou, X., Qu, P., Wang, S., Li, J., Li, F., Wang, L., Hu, Y., 2022. Evaluation of material reuse degree in additive manufacturing by the improved resolution coefficient grey correlation method. *Process Saf. Environ. Prot.* 166, 451–460. <https://doi.org/10.1016/j.psep.2022.08.026>.
- Hao, Y., Yang, W., Yin, K., 2023. Novel wind speed forecasting model based on a deep learning combined strategy in urban energy systems. *Expert Syst. Appl.* 219, 119636. <https://doi.org/10.1016/j.eswa.2023.119636>.
- Hochreiter, S., Schmidhuber, J., 1997. Long short-term memory. *Neural Comput.* 9 (8), 1735–1780. <https://doi.org/10.1162/neco.1997.9.8.1735>.
- Iliyasu, J., Abubakar, A.B., Mamman, S.O., Ahmed, U.A., 2025. Geopolitical risks and price exuberance in European natural gas market. *Energy Res. Lett.* 6 (4), 123310. <https://doi.org/10.46557/001c.123310>.
- Javid, M., Khan, F.N., Arif, U., 2022. Income and price elasticities of natural gas demand in Pakistan: a disaggregated analysis. *Energy Econ.* 113, 106203. <https://doi.org/10.1016/j.eneco.2022.106203>.
- Jiang, P., Nie, Y., Wang, J., Huang, X., 2023. Multivariable short-term electricity price forecasting using artificial intelligence and multi-input multi-output scheme. *Energy Econ.* 117, 106471. <https://doi.org/10.1016/j.eneco.2022.106471>.
- Jin, B., Xu, X., 2024. Price forecasting through neural networks for crude oil, heating oil, and natural gas. *Measurement* 1 (1), 100001. <https://doi.org/10.1016/j.measene.2024.100001>.
- Kapoor, G., Wichitakorn, N., 2023. Electricity price forecasting in New Zealand: a comparative analysis of statistical and machine learning models with feature selection. *Appl. Energy* 347, 121446. <https://doi.org/10.1016/j.apenergy.2023.121446>.
- LaPlue, L.D., 2022. Environmental consequences of natural gas wellhead pricing deregulation. *J. Environ. Econ. Manag.* 116, 102728. <https://doi.org/10.1016/j.jeem.2022.102728>.
- Li, J., Wu, Q., Tian, Y., Fan, L., 2021. Monthly Henry Hub natural gas spot prices forecasting using variational mode decomposition and deep belief network. *Energy* 227, 120478. <https://doi.org/10.1016/j.energy.2021.120478>.
- Li, L., Li, J., Li, K., Luo, X., Jiao, J., 2022. Climatic impacts on residential natural gas consumption: evidence from Hefei, China. *Energy Build.* 275, 112488. <https://doi.org/10.1016/j.enbuild.2022.112488>.
- Liang, B., Liu, J., Kang, L.X., Jiang, K., You, J.Y., Jeong, H., et al., 2024. A novel framework for predicting non-stationary production time series of shale gas based on BiLSTM-RF-MPA deep fusion model. *Pet. Sci.* 21 (5), 3326–3339. <https://doi.org/10.1016/j.petsci.2024.05.012>.
- Lin, Y., Lu, Q., Tan, B., Yu, Y., 2022. Forecasting energy prices using a novel hybrid model with variational mode decomposition. *Energy* 246, 123366. <https://doi.org/10.1016/j.energy.2022.123366>.
- Liu, G., Yu, J., 2007. Gray correlation analysis and prediction models of living refuse generation in Shanghai city. *Waste Manag.* 27 (3), 345–351. <https://doi.org/10.1016/j.wasman.2006.03.010>.
- Malliaris, M.E., Malliaris, S.G., 2008. Forecasting inter-related energy product prices. *Eur. J. Finance* 14, 453–468. <https://doi.org/10.1080/13518470701705793>.
- Mishra, S., Padhy, S., Mishra, S.N., Misra, S.N., 2021. A novel LASSO – TLBO – SVR hybrid model for an efficient portfolio construction. *N. Am. J. Econ. Finance* 55, 101350. <https://doi.org/10.1016/j.najef.2020.101350>.
- Niu, X., Wang, J., 2019. A combined model based on data preprocessing strategy and multi-objective optimization algorithm for short-term wind speed forecasting. *Appl. Energy* 241, 519–539. <https://doi.org/10.1016/j.apenergy.2019.03.097>.
- Niu, T., Wang, J., Lu, H., Yang, W., Du, P., 2020. Developing a deep learning framework with two-stage feature selection for multivariate financial time series forecasting. *Expert Syst. Appl.* 148, 113237. <https://doi.org/10.1016/j.eswa.2020.113237>.

- Niu, X., Wang, J., Zhang, L., 2022. Carbon price forecasting system based on error correction and divide-conquer strategies. *Appl. Soft Comput.* 118, 107935. <https://doi.org/10.1016/j.asoc.2021.107935>.
- Park, H.J., Kim, Y., Kim, H.Y., 2022. Stock market forecasting using a multi-task approach integrating long short-term memory and the random forest framework. *Appl. Soft Comput.* 114, 108106. <https://doi.org/10.1016/j.asoc.2021.108106>.
- Perifanis, T., Dagoumas, A., 2021. Crude oil price determinants and multi-sectoral effects: a review. *Energy sources. Energy Sources B Energy Econ. Plann.* 16, 787–860. <https://doi.org/10.1080/15567249.2021.1922956>.
- Prasad, R., Ali, M., Kwan, P., Khan, H., 2019. Designing a multi-stage multivariate empirical mode decomposition coupled with ant colony optimization and random forest model to forecast monthly solar radiation. *Appl. Energy* 236, 778–792. <https://doi.org/10.1016/j.apenergy.2018.12.034>.
- Shehadeh, H.A., 2023. Chernobyl disaster optimizer (CDO): a novel meta-heuristic method for global optimization. *Neural Comput. Appl.* 35, 10733–10749. <https://doi.org/10.1007/s00521-023-08261-1>.
- Shi, X., Shen, Y., 2021. Macroeconomic uncertainty and natural gas prices: revisiting the Asian Premium. *Energy Econ.* 94, 105081. <https://doi.org/10.1016/j.eneco.2020.105081>.
- Shi, H., Wei, A., Xu, X., Zhu, Y., Hu, H., Tang, S., 2024. A CNN-LSTM based deep learning model with high accuracy and robustness for carbon price forecasting: a case of Shenzhen's carbon market in China. *J. Environ. Manag.* 352, 120131. <https://doi.org/10.1016/j.jenvman.2024.120131>.
- Su, M., Zhang, Z., Zhu, Y., Zha, D., 2019. Data-driven natural gas spot price forecasting with least squares regression boosting algorithm. *Energies* 12 (6), 1094. <https://doi.org/10.3390/en12061094>.
- Sun, S., Jin, F., Li, H., Li, Y., 2021. A new hybrid optimization ensemble learning approach for carbon price forecasting. *Appl. Math. Model.* 97, 182–205. <https://doi.org/10.1016/j.apm.2021.03.020>.
- Tian, G., Peng, Y., Meng, Y., 2023. Forecasting crude oil prices in the COVID-19 era: can machine learn better? *Energy Econ.* 125, 106788. <https://doi.org/10.1016/j.eneco.2023.106788>.
- Tibshirani, R., 1996. Regression shrinkage and selection via the lasso. *J. Roy. Stat. Soc. B* 58 (1), 267–288. <https://doi.org/10.1111/j.2517-6161.1996.tb02080.x>.
- Wang, J., Du, P., Niu, T., Yang, W., 2017. A novel hybrid system based on a new proposed algorithm—Multi-objective whale optimization algorithm for wind speed forecasting. *Appl. Energy* 208, 344–360. <https://doi.org/10.1016/j.apenergy.2017.10.031>.
- Wang, J., Cao, J., Yuan, S., Cheng, M., 2021. Short-term forecasting of natural gas prices by using a novel hybrid method based on a combination of the CEEMDAN-SE and the PSO-ALS-optimized GRU network. *Energy* 233, 121082. <https://doi.org/10.1016/j.energy.2021.121082>.
- Wang, L., Wang, X., Liang, C., 2024. Natural gas volatility prediction via a novel combination of GARCH-MIDAS and one-class SVM. *Q. Rev. Econ. Finance* 98, 101927. <https://doi.org/10.1016/j.qref.2024.101927>.
- Wu, C., Wang, J., Hao, Y., 2022. Deterministic and uncertainty crude oil price forecasting based on outlier detection and modified multi-objective optimization algorithm. *Resour. Policy* 77, 102780. <https://doi.org/10.1016/j.resourpol.2022.102780>.
- Xia, X., Li, A., 2024. Global Natural Gas Market and Changing Trends of Natural Gas Trade. In: China International United Petroleum & Chemicals Co., Ltd., Chinese Academy of Social Sciences, Peking University (eds) Annual Report on China's Petroleum, Gas and New Energy Industry (2022–2023). Current Chinese Economic Report Series. Springer, Singapore. https://doi.org/10.1007/978-981-99-7289-0_9.
- Xian, H., Che, J., 2022. Unified whale optimization algorithm based multi-kernel SVR ensemble learning for wind speed forecasting. *Appl. Soft Comput.* 130, 109690. <https://doi.org/10.1016/j.asoc.2022.109690>.
- Xiao, L., Shao, W., Wang, C., Zhang, K., Lu, H., 2016. Research and application of a hybrid model based on multi-objective optimization for electrical load forecasting. *Appl. Energy* 180, 213–233. <https://doi.org/10.1016/j.apenergy.2016.07.113>.
- Xie, G., Jiang, F., Zhang, C., 2023. A secondary decomposition-ensemble methodology for forecasting natural gas prices using multisource data. *Resour. Policy* 85, 104059. <https://doi.org/10.1016/j.resourpol.2023.104059>.
- Xing, Q., Wang, J., Lu, H., Wang, S., 2022. Research of a novel short-term wind forecasting system based on multi-objective Aquila optimizer for point and interval forecast. *Energy Convers. Manag.* 263, 115583. <https://doi.org/10.1016/j.enconman.2022.115583>.
- Xing, Q., Huang, X., Wang, J., Wang, S., 2024. A novel multivariate combined power load forecasting system based on feature selection and multi-objective intelligent optimization. *Expert Syst. Appl.* 244, 122970. <https://doi.org/10.1016/j.eswa.2023.122970>.
- Xu, Y., Liu, T., Fang, Q., Du, P., Wang, J., 2025. Crude oil price forecasting with multivariate selection, machine learning, and a nonlinear combination strategy. *Eng. Appl. Artif. Intell.* 139, 109510. <https://doi.org/10.1016/j.engappai.2024.109510>.
- Yang, L., Gao, T., Lu, Y., Duan, J., Liu, T., 2023a. Neural network stochastic differential equation models with applications to financial data forecasting. *Appl. Math. Model.* 115, 279–299. <https://doi.org/10.1016/j.apm.2022.11.001>.
- Yang, W., Hao, M., Hao, Y., 2023b. Innovative ensemble system based on mixed frequency modeling for wind speed point and interval forecasting. *Inf. Sci.* 622, 560–586. <https://doi.org/10.1016/j.ins.2022.11.145>.
- Yao, Z., Wang, Z., Wang, D., Wu, J., Chen, L., 2023. An ensemble CNN-LSTM and GRU adaptive weighting model based improved sparrow search algorithm for predicting runoff using historical meteorological and runoff data as input. *J. Hydrol.* 625 (A), 129977. <https://doi.org/10.1016/j.jhydrol.2023.129977>.
- Yarlagadda, B., Iyer, G., Binsted, M., Patel, P., Wise, M., McLeod, J., 2024. The future evolution of global natural gas trade. *iScience* 27 (2), 108902. <https://doi.org/10.1016/j.isci.2024.108902>.
- Zhang, Y., Yao, X., Wu, Q., Huang, Y., Zhou, Z., Yang, J., Liu, X., 2021. Turbidity prediction of lake-type raw water using random forest model based on meteorological data: a case study of Tai lake, China. *J. Environ. Manag.* 290, 112657. <https://doi.org/10.1016/j.jenvman.2021.112657>.
- Zhang, S., Wu, H., Wang, J., Du, L., 2025. Hybrid deep learning for gas price prediction using multi-factor and temporal features. *IEEE Access* 13, 11989–12001. <https://doi.org/10.1109/ACCESS.2024.3525128>.
- Zheng, Y., Luo, J., Chen, J., Chen, Z., Shang, P., 2023. Natural gas spot price prediction research under the background of Russia-Ukraine conflict - based on FS-GA-SVR hybrid model. *J. Environ. Manag.* 344, 118446. <https://doi.org/10.1016/j.jenvman.2023.118446>.
- Ziel, F., Weron, R., 2018. Day-ahead electricity price forecasting with high-dimensional structures: univariate vs. multivariate modeling frameworks. *Energy Econ.* 70, 396–420. <https://doi.org/10.1016/j.eneco.2017.12.016>.